Assessment and Characterization of REE Minerals from an Alkali-Carbonatitic Complex

Juliana Lívi Antoniassi, Daniel Uliana, Henrique Kahn, M. Manuela M. Lé Tassinari, and Carina Ulsen

Abstract The demand for rare earth elements (REE) in high technology industries has been intensified and coupled with the fact that China accounts for about 95 % of world production and is actually creating trade restrictions for these elements; the search for new resources has been encouraged in several countries. This chapter presents a methodology for characterizing an earth rare mineralized sample, which occurs in association with alkali-carbonated complexes and with fine-grained monazite. The procedure was conducted by an automated image analysis system, besides physical separations and selective comminution by scrubbing, thereby evaluating the possibility of enrichment of rare earth bearing minerals in the attained products. Monazite is the main REE bearing mineral, counting for 40 % of the total content; it usually occurs in aggregates with micrometric crystals often with cerianite intergrowth. Monazite is mostly associated with anatase and Fe-oxy-hydroxides presenting a very poor liberation (34 wt% on average for material grinded below 0.30 mm). Both mineral separations and selective grinding by scrubbing did not succeed to obtain products with significant enrichment in REE.

Keywords Rare earth elements • Applied mineralogy • Automated mineralogy • Monazite

1 Introduction

New attention has been given to rare earth minerals resources over the last years. The trade restrictions recently imposed by China and the growing demand for rare earth elements (REE) in high technology industries have motivated the Brazilian Government to encourage new projects by inserting the exploitation of REE in the National Mining Plan, which deals with industry strategic issues in the country and

J.L. Antoniassi (✉) • D. Uliana • H. Kahn • M.M.M.L. Tassinari • C. Ulsen
Mining and Petroleum Engineering Department, Polytechnic School, University of Sao Paulo, Av. Prof. Mello Moraes, 2373 Sao Paulo, SP, Brazil
e-mail: juliana@lct.poli.usp.br

F. Dong (ed.), *Proceedings of the 11th International Congress for Applied Mineralogy (ICAM)*, Springer Geochemistry/Mineralogy,
DOI 10.1007/978-3-319-13948-7_18

helps to reduce current importation. The incentives can be in the choice of future targets for mineral exploration and for the development of laboratory studies and pilot scale processing tests [1, 2].

Although in Brazil there is almost no large-scale exploitation of rare earth minerals, the existing resources are significant and occur mainly in association with alkali-carbonatitic complexes. In these deposits there are several rare earth bearing minerals and monaziteis, the one that has greater resources and potential for exploitation, usually present at extremely fine grain sizes [3, 4].

Because of textural features, fine grain sizes, and complex associations, the technological feasibility of REE depends primarily on the detailed applied mineralogy studies, focus on better understanding of the ore characteristics, processing limitations, and possible stages of physical concentration [5, 6].

This chapter presents a typical and recent applied mineralogical study, developed on a lateritic rare earth ore sample from Brazil, aiming to determinate the mineralogical composition and associations, liberation degree, partition of the rare earth oxides (REO), and its potential recovery, defined by SEM-based automated image analysis (MLA) [7], providing support and parameters for the mineral beneficiation process. Physical separations by density and magnetic susceptibility, as well as selective comminution by scrubbing were also developed, thereby evaluating the possibility of enrichment of rare earth bearing minerals in the attained products.

2 Materials and Methods

2.1 Studied Sample

The studies were performed on a low-grade lateritic rare earth mineralized sample from one of the alkali-carbonatitic complexes in Minas Gerais State, Brazil.

2.1.1 General Characterization Studies

The experimental procedure was adopted for the characterization studies, which comprises:

Homogenization and sampling;
Desliming of a representative aliquot through a 25 mm hydrocyclone (estimated cut off in 0.008 mm) to remove the natural fines from sample;
Grinding of deslimed fraction below 0.30 mm in a rod mill, followed by a second desliming to remove the generated fines by grinding;
Sieve size analyzed by wet screening with screen apertures of 0.21, 0.15, 0.074, 0.037, and 0.020 mm;
Chemical analyses at sieve fractions and in the bulk sample;

Detailed mineralogical studies were conducted by SEM-based automated image analysis and by X-ray diffraction.

2.1.2 Exploratory Mineral Separations and Selective Comminution by Scrubbing

Mineral separations were conducted by a Davis Tube magnetic separator followed by heavy liquid separation (di-methylene iodide—3.30 g/cm^3), aiming to obtain products enriched in rare earth minerals. These assays were performed in all fractions size above 0.008 mm and obtained in general characterization studies. Additionally, selective comminution by scrubbing tests was held on not comminuted aliquots as described below.

Desliming of a representative aliquot through a 25 mm hydrocyclone coupled with two stages (estimated cut off in 0.008 and 0.005 mm) to remove the natural fines from sample;
Scrubbing of material above 0.008 mm in a Denver D12 1,0L cell, considering a 50 % of solids, during 10 min at 1,200 rpm; this assay was followed by a second desliming to remove the fines generated by scrubbing;
Sieve size analysis by wet screening with screen apertures of 0.60, 0.30, 0.15, 0.074, 0.037, and 0.020 mm;
Chemical analyses at sieve fractions and in the bulk sample;
To repeat the desliming and sieve size analysis for a not scrubbed aliquot.

The proposed method is based on the strong and natural tendency of the monazite to break up easily and consequently to concentrate in the finest size fraction, as discussed by Tassinari et al. [4].

2.2 Methods for Assessment and Analysis

2.2.1 Chemical Analysis (X-ray Fluorescence)

Quantitative chemical analysis were carried out by X-ray fluorescence (XRF) in fused pellets, by means of Axios Advanced spectrometer (PANalytical) with determination of CeO_2, La_2O_3, Nd_2O_3, and Pr_2O_3 (REO), besides Nb_2O_5, P_2O_5, CaO, SiO_2, Al_2O_3, Fe_2O_3, MgO, TiO_2, BaO, MnO, and SO_3. Loss on ignition (LOI) was also performed by sample calcinations in a muffle furnace at 1,050 °C for 1 h.

2.2.2 X-ray Diffraction

The mineralogical analysis by X-ray diffraction (XRD) was performed by the powder method in X-ray diffractometer X'Pert PRO with X'Celerator detector (PANalytical). The identification of crystalline phases was obtained by comparing

the diffraction patterns with the database ICDD—International Centre for Diffraction Data.

2.2.3 SEM-Based Automated Mineralogy

The study by scanning electron microscopy (SEM) was carried out in polished sections, previously coated with a carbon film. The qualitative and semi quantitative evaluation of chemical elements presented in the several minerals was accomplished by Stereoscan 440 microscope (LEO) with energy dispersive spectrometer (EDS, Oxford) with an SDD detector and INCA microanalysis system (Oxford). The mineralogical composition of the samples and the partition of the main elements in the bearing minerals were performed through automated image analysis software (Mineral Liberation Analyzer—MLA) coupled with a scanning electron microscope Quanta 600 FEG (FEI) with EDS (Bruker) and microanalysis system Esprit (Bruker). The automated search routine was held by XBSE mode, considering such the atomic number contrast as the chemical composition of each mineral phase (backscattered electrons images and characteristic X-ray spectra by EDS). The chemical and morphological variability of the bearing rare earth minerals was also obtained, taking into account X-ray mapping of the main chemical elements and detail images (1,000–15,000 times magnification).

3 Results

3.1 Chemical Composition

The chemical composition of the sample is presented in Table 1 and the REO total grade is 1.25 wt% (0.63 % of CeO_2, 0.40 % of La_2O_3, and 0.22 % of Nd_2O_3).

High grades of Fe_2O_3 and TiO_2 reach 35.8 and 30.7 wt% respectively, while the SiO_2 content is 15.7 wt%. In minor amounts are the grades of CaO (4.35 wt%), Al_2O_3 (3.65 wt%), P_2O_5 (1.50 wt%), MgO (1.32 wt%), BaO (0.49 wt%), MnO (0.58 wt%), and Nb_2O_5 (0.11 wt%), besides 3.34 % of LOI.

3.2 Particle Size Analysis

Particle size cumulative distribution curves for weight, REO, P_2O_5, SiO_2, Fe_2O_3, and TiO_2 are presented in Fig. 1 for the material comminuted below 0.30 mm.

The fraction size above 0.008 mm represent 83 wt% of the total mass, while 15.8 wt% is relative to the natural fines below 0.008 mm and 1.2 wt% to the fines generated on comminuting process.

Table 1 Bulk sample chemical composition

REO	CeO_2	La_2O_3	Nd_2O_3	Pr_2O_3	Nb_2O_5	P_2O_5	CaO	SiO_2	Al_2O_3	Fe_2O_3	MgO	TiO_2	BaO	MnO	SO_3	LOI	REO/P_2O_5	CaO/P_2O_5
1.25	0.63	0.40	0.22	<0.10	0.11	1.50	4.35	15.7	3.65	35.8	1.32	30.7	0.49	0.58	<0.01	3.34	0.83	2.90

REO Sum of rare earth oxides (CeO_2, La_2O_3, Nd_2O_3, Pr_2O_3)

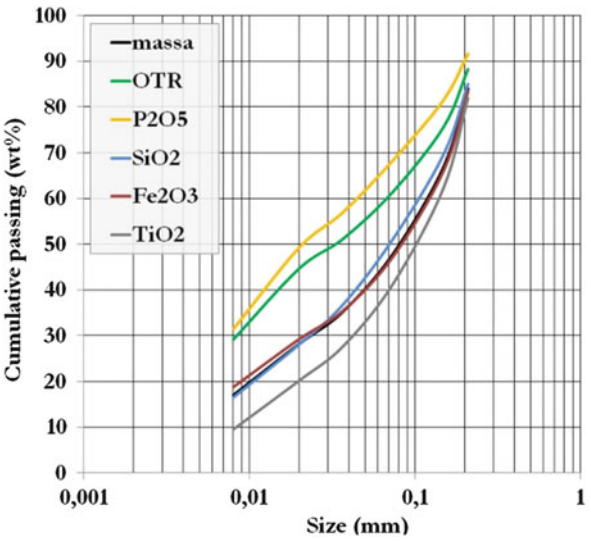

Fig. 1 Weight and main elements distributions by size

REO grades vary from 0.93 to 1.76 wt% above 0.008 mm, increasing to the fine fractions, whereas in the natural fines, this value is 2.18 wt% (27 % of REO total contained in the sample) and reach 2.28 wt% on generated fines (2.1 % of REO total contained).

Among the REO total content, the CeO_2 values are the highest which ranging from 0.50 to 1.17 wt%; the La_2O_3 grades are between 0.28 and 0.66 wt%, the Nd_2O_3 between 0.14 and 0.50 wt%, while the Pr_2O_3 vary between 0.10 and 0.17 wt % in the fractions below 0.037 mm and is less than 0.10 wt% above.

3.3 Mineral Modal Composition

The mineralogical composition of the sample (total -0.30 mm) is represented in the Fig. 2. The major constituents are iron oxy-hydroxides (31 wt%; goethite, hematite and magnetite), anatase (21 wt%), quartz (13 wt%), ilmenite (11 wt%), as well as perovskite (9.0 wt%), clay minerals (8.7 wt%; gibbsite and kaolinite), and Al-phosphates (3.4 wt%; gorceixite–goyazite).

Monazite represents 0.9 wt% of sample with proportions varying between 0.2 and 1.2 wt% in fractions sizes above 0.008 mm and reaching 2.4 and 2.8 wt% in the passing natural and generated material, respectively. Other minerals are also presented with proportions below 1 wt% like Mn-oxide, apatite, zirkelite–zirconolite, baddeleyite, titanite, vermiculite, dolomite, cerianite, and Ba-phosphate.

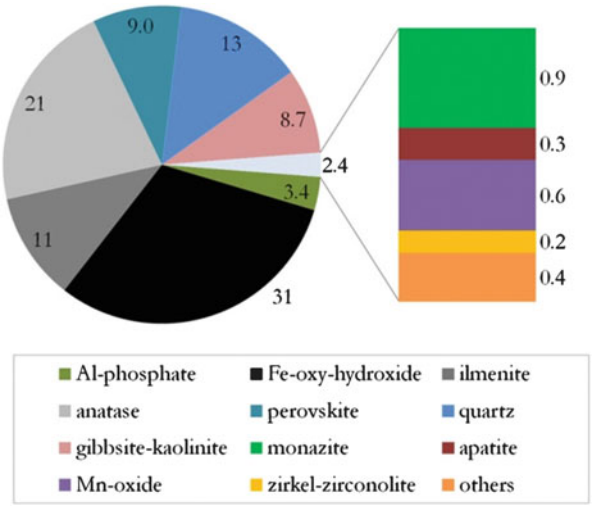

Fig. 2 Mineralogical composition of the studied sample

3.4 Monazite Liberation and Associations

Monazite is the main REO bearing mineral in the sample; usually occurs in aggregates of monazite often with cerianite intergrowth and shows micrometric crystals. These aggregates may present as massive aspects, colloform, or as acicular crystals.

Monazite is mostly associated with anatase and Fe-oxy-hydroxides and shows some compositional variability ($(Ce,REE)PO_4$) and apparently also some hydration (monazite-rhabdophane group), being possible to identify the intergrowth of two predominant types: one richer in lanthanum and another in cerium; this differentiation is not focused in this study.

Monazite aggregates are reached on average 34 wt% of liberation degree by area (particles with >95 % of monazite), varying from 0 to 65 wt% in fractions sizes, gradually increasing towards the fines—Fig. 3. In terms of exposed perimeter (or "free surface" as referred in MLA), the liberation degree is slightly lower due to the trend of gangue minerals concentrating at the border of the locked particles.

It was noticed also the occurrence of submicron inclusions of monazite is preferably associated with anatase and perovskite. The differentiation of these phases depending on the size of these associations sometimes became infeasible for the MLA software to perform a proper mineral classification. So it is expected that the results of monazite quantification may have been slightly underestimated, as well as cerianite and eventually other REO bearing minerals with sub micrometric dimensions may have been added as monazite; on the other side the monazite liberation data are overestimated.

The main features observed for the monazite aggregates are illustrated in Photomicrographs 1 and 2, obtained by SEM/EDS and by elemental mappings.

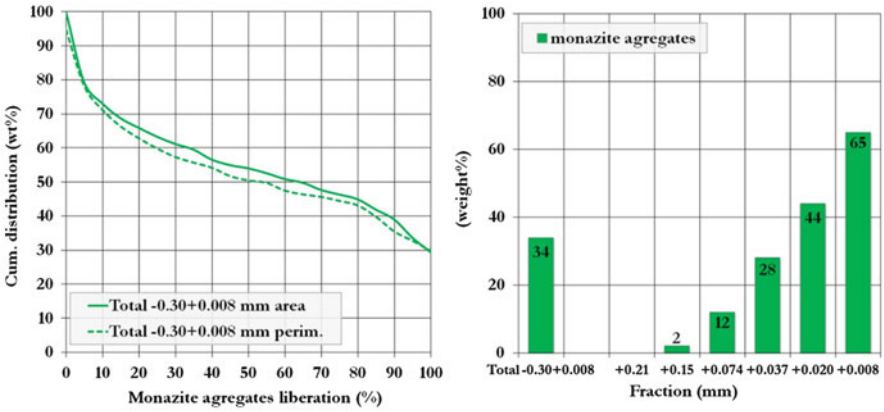

Fig. 3 Liberation degree for the monazite aggregates

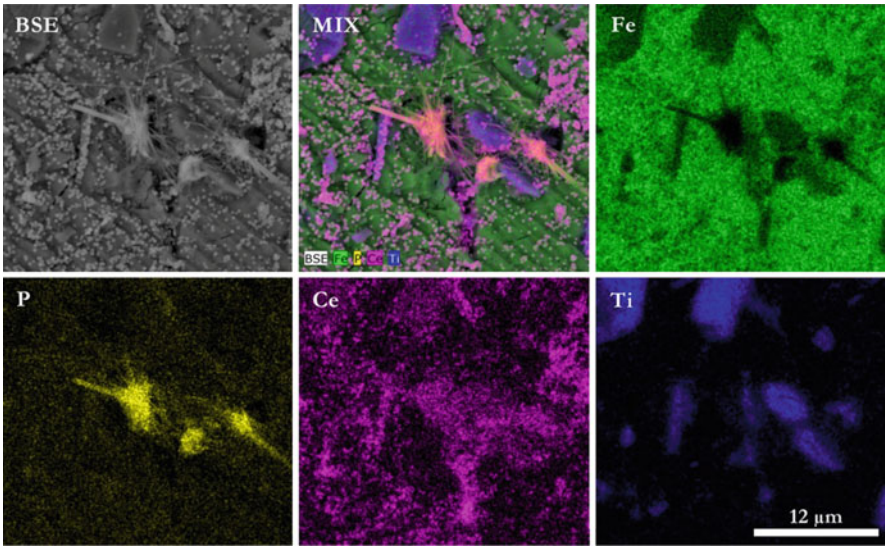

Photomicrograph 1 X-ray elemental mapping obtained by SEM/EDS. Monazite aggregates showing acicular aspect and cerianite as submicron crystals (rounded and porous) associated with Fe-oxide and Ti-oxide

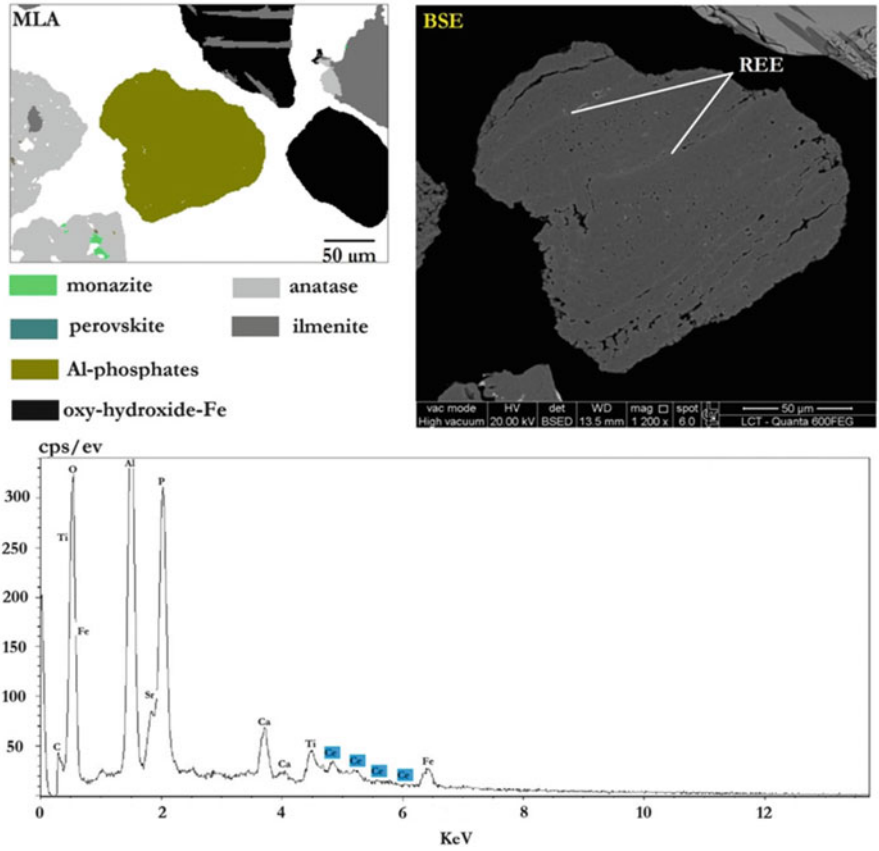

Photomicrograph 2 Free Al-phosphate particle classified by MLA image analysis—gorceixite/goyazite series. Note the presence of veins enriched in REE on the EDS spectrum (not differentiated by MLA in this study)

3.5 Elemental Distribution

The distributions of REO, P_2O_5, CaO, Fe_2O_3, and TiO_2 on bearing minerals are shown in Fig. 4.

Among the REO total content (sum of CeO_2, La_2O_3, Nd_2O_3, and Pr_2O_3), 40 wt% is presented as monazite and cerianite, 4 wt% as Al-phosphates, 1 wt% as zirkelite-zirconolite, 31 wt% is associated with anatase, 11 wt% with iron oxy-hydroxides, 10 wt% with perovskite and 3 wt% with gibbsite–kaolinite. These high contents of REO associated with anatase, iron oxy-hydroxides, perovskite, and others can be also justified by the unclassified submicron REO phases and presented like inclusions as previously mentioned.

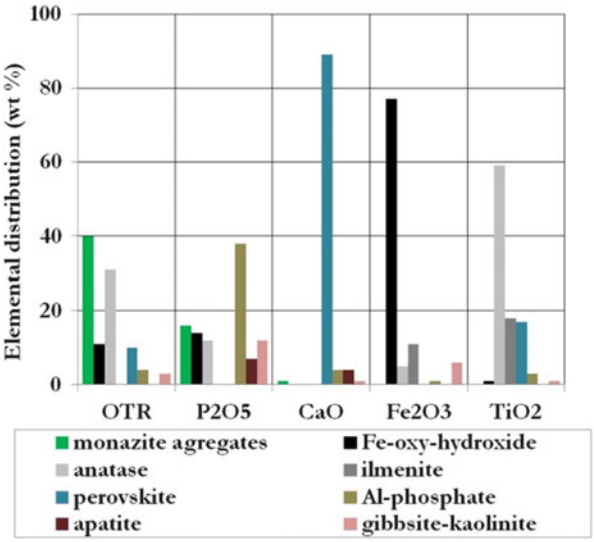

Fig. 4 Distribution of REO-total, P_2O_5, CaO, Fe_2O_3 and TiO_2 among the bearing minerals

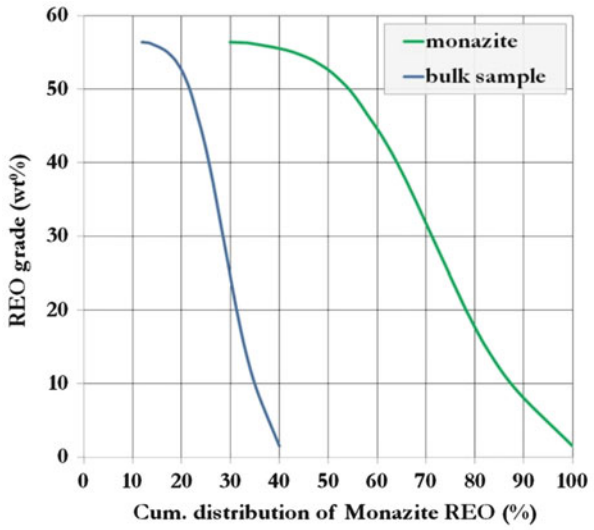

Fig. 5 Distribution of REO-total, P_2O_5, CaO, Fe_2O_3 and TiO_2 among the bearing minerals

3.6 REO Grade Versus Monazite Aggregates Distribution

Considering only the REO is contained in monazite aggregates, the REO grades versus cumulative distribution curves are shown in Fig. 5, indicating a potential recovery of 54 wt% of monazite with a 50 wt% REO grade for the material grinded in 0.30 mm.

As monazite responding for only 40 wt% of REO total content in the sample (−0.30+0.008 mm), considering a product with the same REO grade in monazite aggregates (50 wt%), the potential recovery of REO is 22 wt% for the bulk sample.

3.7 Mineral Separations

Mineral separation results presenting mass distribution and grades and distribution for REO, P_2O_5, CaO, SiO_2, Al_2O_3, Fe_2O_3, and TiO_2 are summarized in Table 2 for the total fraction size −0.30+0.008 mm.

The results indicated no possibility of obtaining products with significant enrichment in REO through physical separations. The nonmagnetic sink product above 0.008 mm corresponds to 41.6 wt% of the sample and presents 1.73 wt% of REO grade (59.6 % recovery relative to the bulk sample); A high concentration of TiO_2 (53.5 wt%; 72 % of the total present in the sample), Fe_2O_3 (22.5 wt%), and CaO (8.70 wt%; 84.5 % of the total present in the sample) remains associated with this product, besides 2.11 wt% of Al_2O_3, 1.53 wt% of P_2O_5, 0.77 wt% of BaO, 0.74 wt% of MnO, 0.27 wt% of Nb_2O_5, and loss on ignition of 3.36 %.

3.8 Selective Comminution by Scrubbing

Cumulative distribution curves for weight, REO, P_2O_5, SiO_2, Fe_2O_3, and TiO_2 are presented in Fig. 6, considering particle size distributions of the original sample and after the scrubbing (selective scrubbing).

Despite increasing the weight to the fine fractions, the REO content in the fines generated after 10 min of scrubbing is almost the same with the natural fines (below 0.008 mm) with no proper evidence of a selective comminution of the monazite aggregates.

Table 2 Summary of the mineral separation results

Product/assay	Fraction (mm)	Weight (wt%)	Grades (wt%)							Distribution (wt%)					
			REO	P_2O_5	CaO	SiO_2	Al_2O_3	Fe_2O_3	TiO_2	REO	P_2O_5	CaO	Al_2O_3	Fe_2O_3	TiO_2
Bulk sample	Total −0.30	100.0	1.25	1.50	4.35	15.7	3.65	35.8	30.7	100.0	100.0	100.0	100.0	100.0	100.0
Float ($d < 3.30$ g/cm^3)	−0.30 +0.008	20.4	0.51	1.92	1.10	56.5	4.39	14.0	13.8	8.5	24.6	5.2	24.2	8.0	9.0
Magnetic (Davis Tube)		21.0	0.15	0.25	1.43	...	0.44	79.3	13.8	2.7	3.4	7.0	2.6	46.9	9.4
Sink ($d > 3.30$ g/cm^3)		41.6	1.73	1.53	8.70	...	2.11	22.5	53.5	59.6	40.6	84.5	24.5	26.3	72.0
Fines	−0.008 natural	15.8	2.18	2.87	0.67	14.7	11.40	41.6	15.0	27.0	29.6	2.5	47.6	18.0	7.8
	−0.008 generated	1.2	2.28	2.33	2.69	15.2	3.42	22.3	44.9	2.1	1.8	0.7	1.1	0.7	1.8

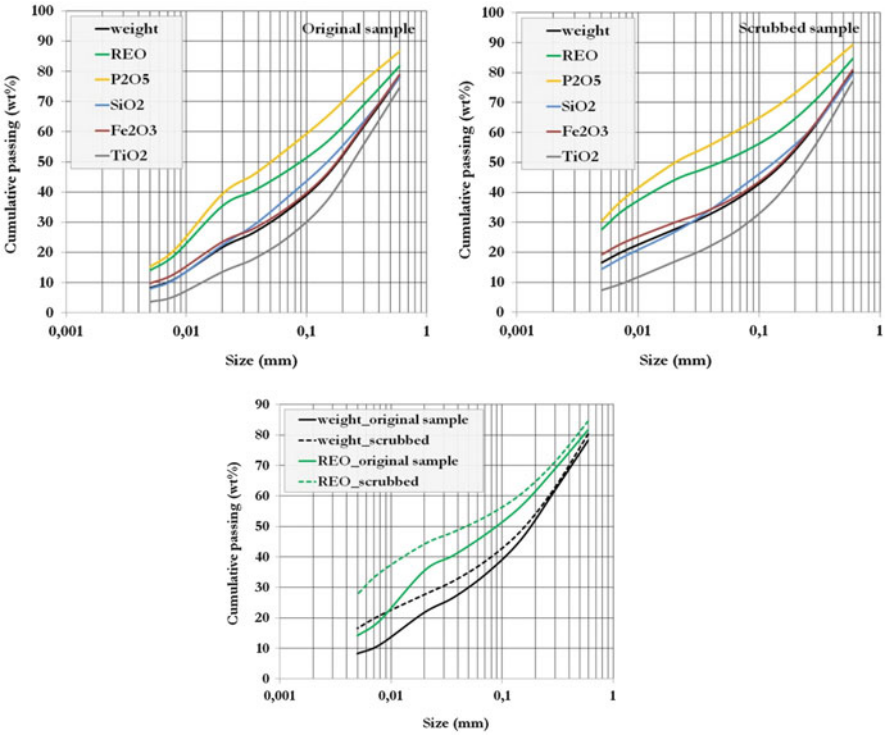

Fig. 6 Weight and main elements distributions by size, considering the original sample and the same scrubbed

4 Final Considerations

The studied sample founded in a Brazilian alkali-carbonatitic complex presents 1.65 % of REO wt%, being 70.8 % presented above 0.008 mm fraction. Monazite aggregates are the main REO bearing mineral and show a poor liberation above this fraction (only 34 wt%); due to monazite associations, mineral separations were not effective in obtaining products with higher enrichments in rare earth oxides. Because fractions below 0.008 mm, even with grinding and scrubbing assays, the grades of REO did not exceed 2.2 wt% in the fine products generated. The only remaining alternative is to evaluate hydrometallurgical tests by sulphuric acid leaching at low temperatures.

Acknowledgments The authors acknowledge the financial support of FAPESP—Sao Paulo Research Foundation, process 2009-54007-0 to carry out this research.

References

1. Guerra R (2013) Comitê define prioridades para aplicar orçamento do setor mineral. MCTI—Ministério da Ciência, Tecnologia e Inovação, Brasil
2. Rocio MAR, Silva MM, Carvalho PSL, Cardoso JGR (2012) Terras raras: situação atual e perspectivas. Banco Nacional do desenvolvimento, Brasil. BNDES setorial: Mineração 35:369–420
3. Kahn H, Tassinari MMML, Ulsen C, Uliana D (2012) Terras Raras—Monazita associada a complexos alcalino-carbonatíticos. Revista ABM Metalurgia, Materiais & Mineração 38:125–129
4. Tassinari MMML, Kahn H, Ratti G (2001) Process mineralogy studies of Córrego do Garimpo REE ore, Catalão-I alkaline complex, Goiás, Brazil. Miner Eng 14(12):1609–1617
5. Mariano AN (1989) Economic geology of rare earth minerals. In: Lipin BR, McKay GA (eds) Geochemistry and mineralogy of rare earth elements, vol 21. Reviews in Mineralogy, pp 309–337
6. Viera EV, Lins FAF (1997) Concentração de minérios de terras-raras: uma revisão. Rio de Janeiro: CETEM/CNPq. Série Tecnologia Mineral 73, p 53
7. Fandrich R, Ying G, Debra B, Kurt M (2007) Modern SEM-based mineral liberation analysis. Int J Miner Process 84:310–320